Applied Catalysis B: Environmental 147 (2014) 394–401

Contents lists available at ScienceDirect

Applied Catalysis B: Environmental

journal homepage: www.elsevier.com/locate/apcatb

Palladium(0) nanoparticles supported on metal organic framework as highly active and reusable nanocatalyst in dehydrogenation of dimethylamine-borane

Mehmet Gulcan[a], Mehmet Zahmakiran[a,*], Saim Özkar[b]

[a] Department of Chemistry, Science Faculty, Yüzüncü Yıl University, 65080 Van, Turkey
[b] Department of Chemistry, Middle East Technical University, 06800 Ankara, Turkey

ARTICLE INFO

Article history:
Received 10 June 2013
Received in revised form 31 August 2013
Accepted 6 September 2013
Available online 26 September 2013

Keywords:
Nanocatalyst
Palladium nanoparticles
Metal-organic framework
Dimethylamine-borane
Hydrogen

ABSTRACT

Palladium(0) nanoparticles supported on the external surface of $Cu_3(btc)_2$ framework (PdNPs@$Cu_3(btc)_2$) were *in-situ* generated from the reduction of $Pd(acac)_2$ precursor impregnated on the $Cu_3(btc)_2$ support during the dehydrogenation of dimethylamine-borane in toluene at room temperature. The characterization of PdNPs@$Cu_3(btc)_2$ by using advanced analytical techniques shows the formation of well-dispersed palladium(0) nanoparticles supported on $Cu_3(btc)_2$ surface. These new palladium(0) nanoparticles were found to be the most active and the longest-lived nanocatalyst with superior reusability performance in the dehydrogenation of dimethylamine-borane at room temperature.

© 2013 Elsevier B.V. All rights reserved.

1. Introduction

Today, there is a considerable interest in the fabrication of metal nanoparticles with high stability and controllable size distribution because of their potential applications in many fields [1] including catalysis [2,3]. It is well-known that, the agglomeration of initially well-dispersed nanoparticles throughout the catalytic runs in the reaction solution [4], is still the most important problem in their catalytic applications. At this concern, the stabilization of nanoparticles by the framework of porous solid support materials seems to be one of the possible ways for preventing the agglomeration of nanoparticles in their catalytic use [5]. Of particular interest, the recent studies [6–10] have already demonstrated that metal-organic frameworks (MOFs) can be considered as suitable porous solid materials for the stabilization of ligand-free metal nanoparticles. MOFs can exhibit high surface area as well as tunable pore size by the proper selection of the structural subunits and the connected ways [8], which are the important advantages of their employment as host material for the guest metal nanoparticles with respect to silica based porous materials.

Herein we report the synthesis, characterization and catalytic use of palladium(0) nanoparticles stabilized by the framework of $Cu_3(btc)_2$ (general formula: $Cu_3(btc)_2(H_2O)_3$, btc = benzene-1,3,5-tricarboxylate and also known as HKUST-1 [11] or MOF-199 [12]). $Cu_3(btc)_2$ was selected as the representative microporous metal-organic framework, because of its high thermal stability and chemical resistance [11]. It has a complex three-dimensional channel system. The largest pores are 9 Å in diameter and are formed from 12 dinuclear $Cu_2(OOC)_4$ subunits forming a cuboctahedron. A second pore system is accessible from these larger pores, in which four benzene rings constitute the inner surface with the centers of the rings forming a tetrahedron of diameter 5 Å. It can provide free coordination sites on the Cu(II) ion via dehydration under mild conditions [13,14] and these sites are oriented towards the center of one of the larger pore types [11]. Another key parameter considered in the selection of $Cu_3(btc)_2$ as support materials over the silica-based micro and/or mesoporous materials (zeolite, SBA-15, etc.) is that the dehydration of $Cu_3(btc)_2$ occurs under mild conditions. The silica-based materials usually require harsh conditions (673 K and 10^{-5} Torr vacuum) for the same purpose [14]. It has already been demonstrated that $Cu_3(btc)_2$ can be used as a suitable host material for CuO–CeO_2 [15], Au [16], and PdO_2 nanoparticles [17]. Palladium is a suitable metal enhancing the hydrogen uptake in MOF materials [18,19]. In this study, palladium(0) nanoparticles were generated on $Cu_3(btc)_2$ (PdNPs@$Cu_3(btc)_2$) under *in-situ* conditions during the room temperature dehydrogenation of dimethylamine-borane ($(CH_3)_2NHBH_3$; DMAB) starting with $Pd(acac)_2$@$Cu_3(btc)_2$ precatalyst. The resulting PdNPs@$Cu_3(btc)_2$ was characterized by ICP-MS, EA, P-XRD, XPS, TEM, HRTEM, STEM, STEM/EDX, HAADF/STEM,

* Corresponding author. Tel.: +90 5323034741; fax: +90 4322251806.
E-mail address: zmehmet@yyu.edu.tr (M. Zahmakiran).

0926-3373/$ – see front matter © 2013 Elsevier B.V. All rights reserved.
http://dx.doi.org/10.1016/j.apcatb.2013.09.007

NMR spectroscopies and N_2-adsorption–desorption technique. The sum of their results shows the formation of well-dispersed palladium(0) nanoparticles supported on $Cu_3(btc)_2$ surface. The catalytic performance of these new palladium(0) nanoparticles in terms of activity, lifetime and reusability was tested in dehydrogenation (or dehydrocoupling) of DMAB (**1**), which have been identified as the prominent aspirants for chemical hydrogen storage [20], in toluene under mild conditions (298 K and under Ar).

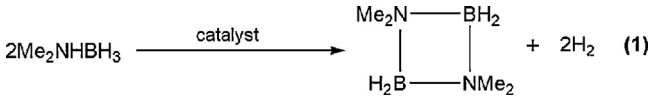

Various homogeneous and heterogeneous catalysts have been tested in dehydrogenation of DMAB [20,21]. Although the record activity has been achieved by using homogeneous [η^5-C_5H_3-1,3-$(SiMe_3)_2Ti]_2(\mu_2,\eta^1,\eta^1$-$N_2)$ catalyst [22], the current research has focused on the development of supported metal nanoparticle catalysts because of their significant advantages in product isolation, catalyst recovery and reusability [2,3]. Up to date, there is only one report [23] came from Manners' group for the employment of supported metal catalyst (skeletal Ni; sponge–metal type = Al/Ni) in the dehydrogenation of DMAB, which provides only low activity with a turnover frequency (TOF) value of 3.2 h^{-1} at complete conversion of DMAB. Additionally, a quick literature search also showed that metal nanoparticles loaded or metal free MOF materials have already been used in the hydrogen generation from ammonia-borane and amine-borane derivatives [24–27].

PdNPs@$Cu_3(btc)_2$ provide the release of 1 equiv. of H_2 per mole of DMAB with an *initial* TOF value of 73 h^{-1} at 298 K, which is a record TOF value among all the heterogeneous catalysts tested in dehydrogenation of DMAB (Table 1). More importantly, PdNPs@$Cu_3(btc)_2$ show high stability against leaching and sintering throughout the catalytic runs, which make them long-lived and reusable catalyst. Consequently, they provide a total turnover number (TTON) of 2100 and retain almost their inherent activity even at the fifth catalytic reuse in the dehydrogenation of DMAB.

2. Experimental

2.1. Materials

Palladium(II) acetylacetonate ($Pd(acac)_2$), copper(II) nitrate trihydrate ($Cu(NO_3)_2{\cdot}3H_2O$), ethanol (C_2H_5OH), toluene (C_7H_8), dimethylamine-borane ($(CH_3)_2NHBH_3$) were purchased from Sigma–Aldrich. Benzene-1,3,5-tricarboxylic acid (trimesic acid; H_3BTC) was purchased from Acros. Dimethylamine-borane was purified by sublimation at 25 °C. Deuterated NMR solvent toluene-d_8 (from Sigma–Aldrich) was transferred into the glovebox for NMR sample preparations therein. Toluene was distilled over sodium under argon atmosphere and stored in the glovebox (O_2 < 5 ppm, H_2O < 1 ppm). All glassware and Teflon coated magnetic stir bars, Teflon-lined steel autoclaves were cleaned with acetone, followed by copious rinsing with distilled water before drying in an oven at 150 °C.

2.2. Characterization

The amount of palladium loaded on $Cu_3(btc)_2$ and leached into the solution were determined by inductively couple plasma mass spectroscopy (ICP-MS) by using Perkin Elmer DRC II model. X-ray diffraction (XRD) analyzes were carried out on Rigaku Ultima-IV in the range of 2θ = 5–60°. NMR spectra were taken on a Bruker Avance DPX 400 MHz spectrometer (400.1 MHz for ^{1}H NMR, 100.8 MHz for ^{13}C NMR, 128.2 MHz for ^{11}B NMR). $Si(CH_3)_4$ was used as the internal reference for ^{1}H and ^{13}C NMR chemical shifts $BF_3{\cdot}(C_2H_5)_2O$ was used as the external reference for ^{11}B NMR chemical shifts. The transmission electron microscopy (TEM), high resolution-TEM (HR-TEM), scanning-TEM (STEM) and high angle annular dark field-STEM (HAADF/STEM) images were taken on JEOL JEM-2010F (FEG, 80–200 kV). Oxford energy dispersive X-ray spectroscopy (EDXS) system and Inca software were used to collect and process STEM/EDX data. X-ray photoelectron spectroscopy (XPS) analyzes were performed on a Physical Electronics 5800 spectrometer equipped with a hemispherical analyzer and using monochromatic Al-Kα radiation (1486.6 eV, the X-ray tube working

Table 1
Pre(catalyst)s tested in the dehyrogenation of dimethylamine-borane under mild conditions (ND, not demonstrated).

Entry	Pre(catalyst)	T (°C)	Conv. (%)	TOF (h^{-1})	Reuse (% retained activity)	Ref.
1	$[Rh(1,5\text{-cod})\mu\text{-Cl}]_2$	25	100	12.4	ND	[41]
2	$[Ir(1,5\text{-cod})\mu\text{-Cl}]_2$	25	95	0.7	ND	[42]
3	$RhCl_3$	25	90	7.9	ND	[42]
4	$IrCl_3$	25	25	0.3	ND	[42]
5	$RhCl(PPh_3)_3$	25	100	4.3	ND	[42]
6	$[Cp^*Rh(\mu\text{-Cl})Cl]_2$	25	100	0.9	ND	[42]
7	$[Rh(1,5\text{-cod})_2]Otf$	25	95	12	ND	[42]
8	$[Rh(1,5\text{-cod})(dmpe)]PF_6$	25	95	1.7	ND	[42]
9	$HRh(CO)(PPh_3)_3$	25	5	0.1	ND	[42]
10	*trans*-$RuMe_2(PMe_3)_4$	25	100	12.4	ND	[42]
11	*trans*-$PdCl_2(P(o\text{-tolyl})_3)_2$	25	20	0.2	ND	[42]
12	Pd/C	25	95	2.8	ND	[42]
13	Cp_2Ti	20	100	12.3	ND	[43]
14	Rh(0)/$[Noct_4]Cl$	25	100	8.2	<25% in the 2nd run	[44]
15	$[C_5H_3\text{-}1,3(SiMe_3)_2)_2Ti]_2$	23	100	420	ND	[22]
16	$[RhCl(PHCy_2)_3]$	20	100	2.6	ND	[45]
17	Rh(0)NPs/Oct	25	100	60	<10% in the 2nd run	[39]
18	$[RuH(PMe_3)(NC_2H_4PPr_2)_2]$	25	100	1.5	ND	[46]
19	(Idipp)CuCl	25	100	0.3	ND	[47]
20	$[Cr(CO)_5(thf)]$	25	97	13.4	ND	[48]
21	$[Cr(CO)_5(\eta^1\text{-}BH_3NMe_3)]$	25	97	19.9	ND	[48]
22	$RuCl_3{\cdot}3H_2O$	25	77	2.7	<5% in the 2nd run	[49]
23	$[Ru(1,5\text{-cod})Cl_2]_n$	25	70	2.5	<5% in the 2nd run	[49]
24	Ru(cod)(cot)	25	40	1.6	<1% in the 2nd run	[49]
25	Ru(0)NPs/APTS	25	100	55	80% in the 3rd run	[50]
26	Ni(skeletal)	20	100	3.2	12% in the 2nd run	[23]
27	**PdNPs@$Cu_3(btc)_2$**	**25**	**100**	**75**	**80% in the 5th run**	**This study**

at 15 kV, 350 W and pass energy of 23.5 keV). The nitrogen adsorption/desorption experiment was carried out at 77 K using a NOVA 3000 series instrument (Quantachrome Instruments). The sample was out-gassed under vacuum at 473 K for 3 h before the adsorption of nitrogen.

2.3. Synthesis of $Cu_3(btc)_2$ and $Pd(acac)_2@Cu_3(btc)_2$

Synthesis of $Cu_3(btc)_2$ was carried out according to slightly modified literature procedures [28,29]. In a typical experiment, a solution of $Cu(NO_3)_2{\cdot}3H_2O$ (4.8 g; 20 mmol) in doubly distilled water (70 mL) was stirred with a solution of H_3BTC (benzene-1,3,5-tricarboxylic acid (trimesic acid; 2.3 g; 11 mmol)) in pure ethanol (70 mL) for half an hour and then divided into four Teflon-lined steel autoclaves (35 mL each). After 14 h at 110 °C, the autoclaves were immediately cooled down to room temperature. The blue precipitate was then filtered off, and washed twice with a mixture of ethanol/water (50:50) and subsequently washed three times with doubly distilled water. The solid product was first dried at 60 °C for 4 h and then overnight at 110 °C.

Typically, 100 mg of activated $Cu_3(btc)_2$ was suspended in 6.0 mL of dry methanol in the Schlenk tube and the mixture was sonicated for 15 min. After stirring of 1 h, 4.0 mL of $Pd(acac)_2$ solution (31.8 mg $Pd(acac)_2$ in methanol) was added dropwise over a period of 15 min with constant vigorous stirring. The resulting solution was continuously stirred for 8 h. After that, the methanol was removed from the suspension under vacuum (10^{-4} Torr) at 353 K. The Schlenk tube containing the solid powder of $Pd(acac)_2@Cu_3(btc)_2$ was transferred into the glovebox. Inside the glovebox, $Pd(acac)_2@Cu_3(btc)_2$ sample was weighed and placed into a new Schlenk tube, which was then, sealed, brought outside the glovebox. The dehydration of $Pd(acac)_2@Cu_3(btc)_2$ sample was done by heating the sample at 423 K under vacuum (10^{-4} Torr) in a stream of argon for 8 h. The activation of $Pd(acac)_2@Cu_3(btc)_2$ by dehydration should be done as the existence of trace of amount of water in the reaction medium shifts the reaction to the hydrolysis of DMAB [13]. The dehydrated sample of $Pd(acac)_2@Cu_3(btc)_2$ was then stored inside the glovebox.

2.4. General procedure for the in-situ formation of $PdNPs@Cu_3(btc)_2$ and the determination of their catalytic activity in the dehydrogenation of dimethylamine-borane

The *in-situ* formation of $PdNPs@Cu_3(btc)_2$ and the concomitant dehydrogenation of DMAB were performed in a Fischer–Porter (F-P) pressure bottle connected to a system that enables us the monitoring of H_2 pressure in F-P bottle on the computer by using the LabVIEW 8.0 program [30]. In a glovebox, 100 mg of $PdNPs@Cu_3(btc)_2$ with 0.86 wt% Pd loading was weighted and transferred into a new 22 mm × 175 mm pyrex culture tube containing a new 5/16 in. × 5/8 in. Teflon coated magnetic stir bar. The culture tube was then sealed inside the F-P bottle, which was brought outside the glovebox and placed inside a constant-temperature circulating water bath thermostated at 298 K unless otherwise specified. Next, the F-P bottle was connected to the line, which had already been evacuated for at least 30 min to remove any trace of oxygen and water present, via its Swagelock TFE-sealed quick connects. Under nitrogen atmosphere, 10 mL of 100 mM DMAB solution (in toluene) was added to the F-P bottle rapidly via tap of bottle by using a cannula technique. When a constant pressure inside the F-P bottle was established, the reaction was started ($t = 0$ min) by stirring the mixture at 900 rpm. When no more hydrogen generation was observed, the experiment was stopped, the F-P bottle was sealed and disconnected from the line, and the hydrogen pressure was released. Then the F-P bottle was transferred back into the glovebox. An approximately 0.5 mL aliquot of the reaction solution in the culture tube was withdrawn with a 9 in. glass Pasteur pipet and added to 1.0 g of $CDCl_3$ in an individual glass ampule. The solution was then transferred into a quartz NMR sample tube (Norell S-500-QTZ), which was subsequently sealed and then brought out of the glovebox for NMR analyzes. ^{13}C and ^{11}B NMR analyzes of the resulting reaction solution showed that the formation of $[Me_2NBH_2]_2$ (^{11}B NMR: 5 ppm; ^{13}C NMR: 52 ppm) and $CH_3CH(OH)CH_2CH(OH)CH_3$ (^{13}C NMR; 60, 47 and 23 ppm).

2.5. Data handling

The catalytic activity of $PdNPs@Cu_3(btc)_2$ was determined by measuring the rate of hydrogen generation. The raw pressure versus time data collected with the computer interfaced transducer were exported from LabVIEW 8.0 and imported into OriginPro 8. The raw data from experiments carried out in toluene were corrected for the build-up of pressure in the F-P bottle due to the solvent vapor pressure and the initial nitrogen pressure was then converted into the values in proper units, volume of hydrogen (mL).

2.6. Control experiment: $Cu_3(btc)_2$ catalyzed dehydrogenation of dimethylamine-borane

In a control experiment the catalytic activity of dehydrated $Cu_3(btc)_2$ (100 mg) was tested in the dehydrogenation of 1 mmol DMAB in toluene (10 mL) at room temperature by following the procedure described in the previous section.

2.7. Isolability, bottlability and reusability of $PdNPs@Cu_3(btc)_2$ in the dehydrogenation of dimethylamine-borane

After the first run of the dehydrogenation of 1.0 mmol of DMAB starting with 100 mg of $Pd(acac)_2@Cu_3(btc)_2$, the FP bottle was detached from the line, taken into the dry-box, the suspension in the culture tube was transferred into a Schlenk tube, resealed and connected to a vacuum line. After the evaporation of volatiles, the solid residue was weighed and used again in the dehydrogenation of 1.0 mmol of DMAB under the same conditions (in 10 mL toluene at 298 K). This procedure was followed up to five catalytic runs.

2.8. Mercury (Hg(0)) poisoning of $PdNPs@Cu_3(btc)_2$

Elemental Hg (0.49 g, ca. 300 equiv.) was added into a 5 mL solution containing 100 mg $PdNPs@Cu_3(btc)_2$ (with 0.86 wt% Pd loading) in the nitrogen filled dry-box and the mixture stirred for 4 h. Then, this solution was used in the dehydrogenation of 1.0 mmol DMAB under the same conditions given above.

2.9. Catalytic lifetime of $PdNPs@Cu_3(btc)_2$ in the dehydrogenation of dimethylamine-borane

The catalytic lifetime of $PdNPs@Cu_3(btc)_2$ in the dehydrogenation of DMAB was determined by measuring the total turnover number (TTON). This experiment was started with a 100 mg $PdNPs@Cu_3(btc)_2$ (with 0.86 wt% Pd loading corresponds to 8.1 μmol) in 10 mL toluene solution of 300 mM DMAB. When the complete conversion is achieved, more DMAB was added into the solution and the reaction was continued in this way until no hydrogen gas evolution was observed.

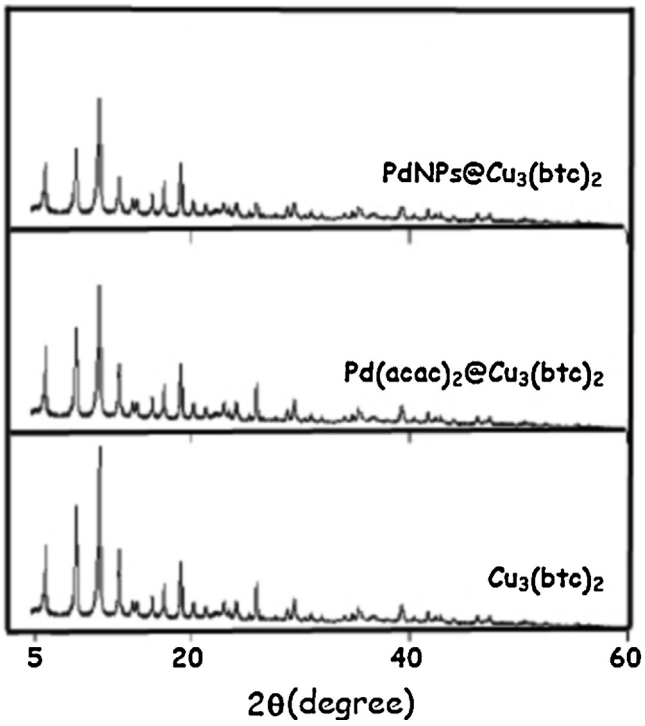

Fig. 1. Powder X-ray diffraction (P-XRD) patterns of $Cu_3(btc)_2$, $Pd(acac)_2@Cu_3(btc)_2$ and $PdNPs@Cu_3(btc)_2$ with a palladium loading of 0.86 wt%.

3. Results and discussion

3.1. Preparation and characterization of palladium(0) nanoparticles supported on $Cu_3(btc)_2$ framework ($PdNPs@Cu_3(btc)_2$)

Palladium nanoparticles (PdNPs) supported on $Cu_3(btc)_2$ framework, hereafter referred to as $PdNPs@Cu_3(btc)_2$, were prepared by following the procedure comprising of (i) wet-impregnation of $Pd(acac)_2$ on $Cu_3(btc)_2$ ($Pd(acac)_2@Cu_3(btc)_2$), (ii) the dehydration of $Pd(acac)_2@Cu_3(btc)_2$, (iii) the *in-situ* reduction of $Pd(acac)_2@Cu_3(btc)_2$ during the room temperature dehydrogenation of DMAB. $PdNPs@Cu_3(btc)_2$ can be isolated as powder by evaporation of solvent and drying under inert atmosphere. The XRD patterns of $Pd(acac)_2@Cu_3(btc)_2$ and $PdNPs@Cu_3(btc)_2$ (containing 0.86 wt% Pd as determined by ICP-MS) are identical with that of $Cu_3(btc)_2$ (Fig. 1). Any impurities or other phases are not observed, indicating that the host material remains intact at the end of the procedure without observable alteration in the framework lattice and loss in the crystallinity.

The size, morphology and local composition of $PdNPs@Cu_3(btc)_2$ were investigated by TEM, HRTEM, STEM, STEM/EDX and HAADF/STEM. TEM image of $PdNPs@Cu_3(btc)_2$ (Fig. 2(a)) shows the presence of well dispersed palladium(0) nanoparticles of the size 4.3 ± 1.1 nm (Fig. 2(b)) supported on $Cu_3(btc)_2$. The formation of palladium(0) nanoparticles of the size 3.4–5.5 nm on the external surface of metal organic framework is expected since the channels diameter and the aperture to the channels of $Cu_3(btc)_2$ are too small for the formation of such particles (the channel diameter and the aperture are 1.32 and 0.9 nm for the large cages and 0.6 and 04.6 nm for the small cages, respectively) [11–14]. HRTEM image of these palladium(0) nanoparticles shown in Fig. 2(c) reveals the highly crystalline feature of the particles with a crystalline spacing of 0.20 nm, which agrees with the [2 0 0] lattice spacing of face centered cubic (fcc) palladium [31].

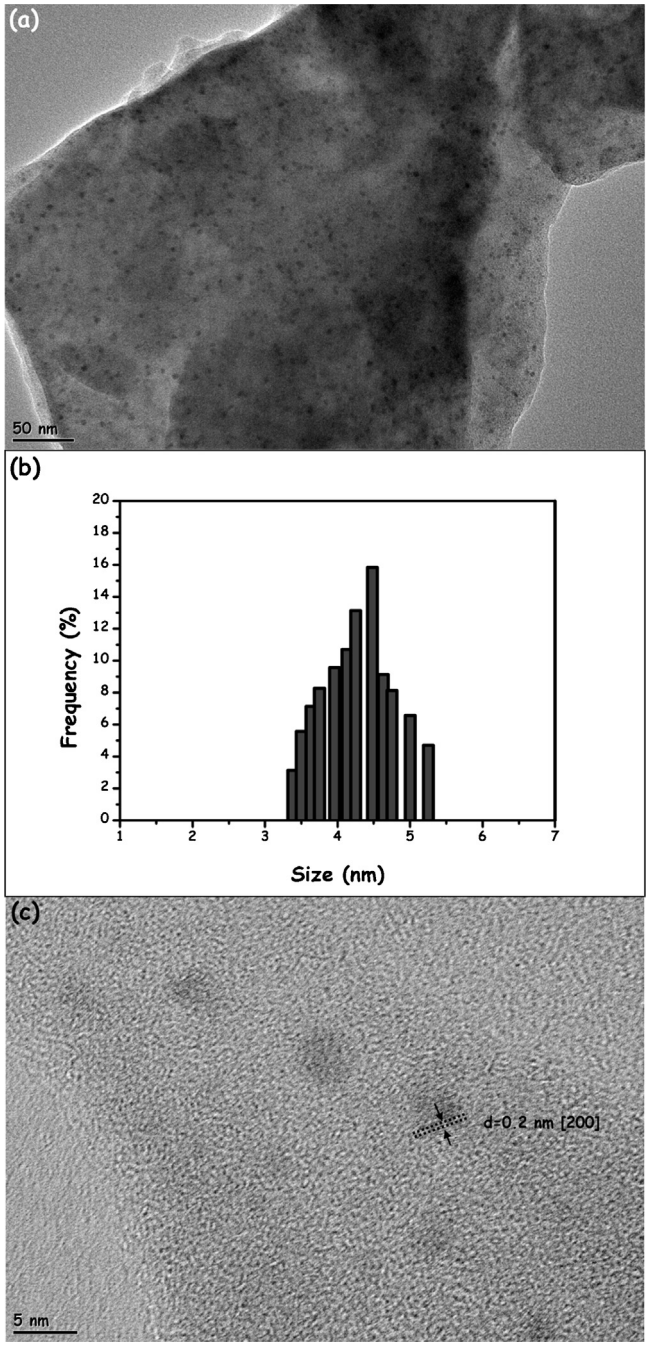

Fig. 2. (a) TEM image of $PdNPs@Cu_3(btc)_2$, (b) size histogram of palladium nanoparticles constructed from counting > 100 particles given in (a), and (c) high resolution TEM (HRTEM) image of $PdNPs@Cu_3(btc)_2$.

The STEM/EDX spectrum of $PdNPs@Cu_3(btc)_2$ (Fig. 3(b)) taken from STEM region given in Fig. 3(a) confirms the existence of Pd in the analyzed region as judged by Lg_1 and Lg_2 lines of Pd in the region of 2.9–3.2 keV [32]. Moreover, Pd-mapped-HAADF/STEM image of $PdNPs@Cu_3(btc)_2$ (Fig. 3(c) inset) is revealing that the well-dispersed PdNPs on $Cu_3(btc)_2$ in the selected region.

The oxidation state of palladium in the resulting $PdNPs@Cu_3(btc)_2$ sample was analyzed by X-ray photoelectron spectroscopy. The high resolution Pd 3d XPS spectrum of $PdNPs@Cu_3(btc)_2$ (Fig. 4) gives two prominent bands at 335.7 and 341.2 eV that are readily assigned to Pd(0) $3d_{5/2}$ and Pd(0)

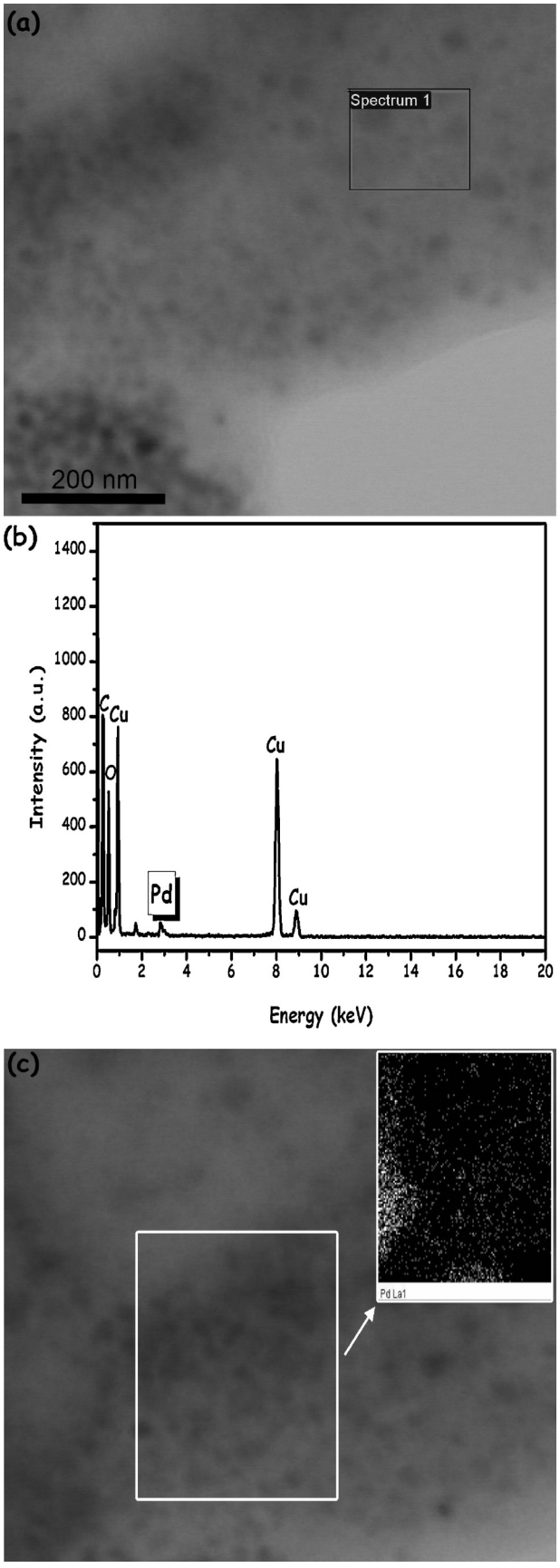

Fig. 3. (a) STEM image of PdNPs@$Cu_3(btc)_2$, (b) STEM/EDX spectrum collected from the region labeled as black rectangle on STEM image given in (a), and (c) STEM image and Pd mapped-HAADF/STEM image collected from the region labeled as white rectangle on STEM image.

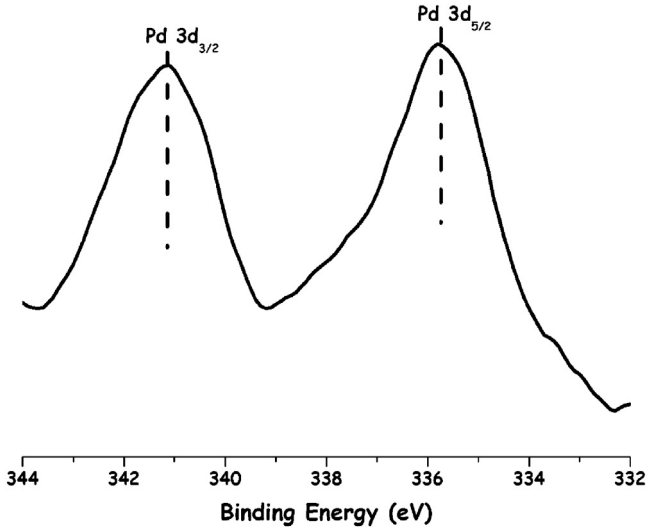

Fig. 4. High resolution Pd 3d XPS spectrum of PdNPs@$Cu_3(btc)_2$ in the region of 344–332 eV.

$3d_{3/2}$ [33] respectively, thus indicating the complete reduction of palladium(II) on the surface of $Cu_3(btc)_2$ matrix to palladium(0) by DMAB during the dehydrogenation. Compared to the value of metallic palladium 3d peaks, the slight shift (ΔE_b = +0.5 eV) observed in PdNPs@$Cu_3(btc)_2$ towards higher energy might be attributed to both the quantum size effect [34] and peculiar electronic properties of the metal organic framework [35,36].

Nitrogen adsorption–desorption isotherms of $Cu_3(btc)_2$ and PdNPs@$Cu_3(btc)_2$ (Fig. 5) show Type I shape, which is a characteristic of the microporous materials [37]. On passing from $Cu_3(btc)_2$ to PdNPs@$Cu_3(btc)_2$, the BET surface area is reduced from 1530 to 1414 m^2/g, which can be attributed to the deposition of PdNPs on the windows of some cavities. Please recall that the electron microscopy analyzes show only the existence of PdNPs supported on the surface of PdNPs@$Cu_3(btc)_2$. Furthermore, no hysteresis loop was observed in the N_2 adsorption–desorption isotherm of PdNPs@$Cu_3(btc)_2$, indicating that the two-step procedure followed in the preparation of PdNPs@$Cu_3(btc)_2$ does not create any mesopores in the $Cu_3(btc)_2$ framework.

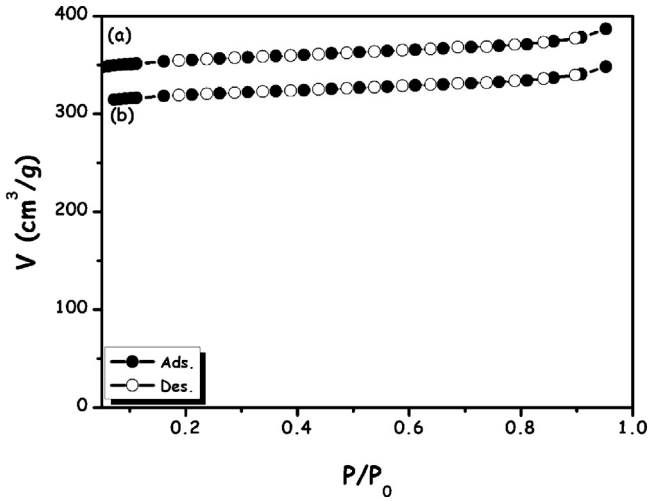

Fig. 5. Nitrogen adsorption–desorption isotherms of (a) $Cu_3(btc)_2$ and (b) PdNPs@$Cu_3(btc)_2$.

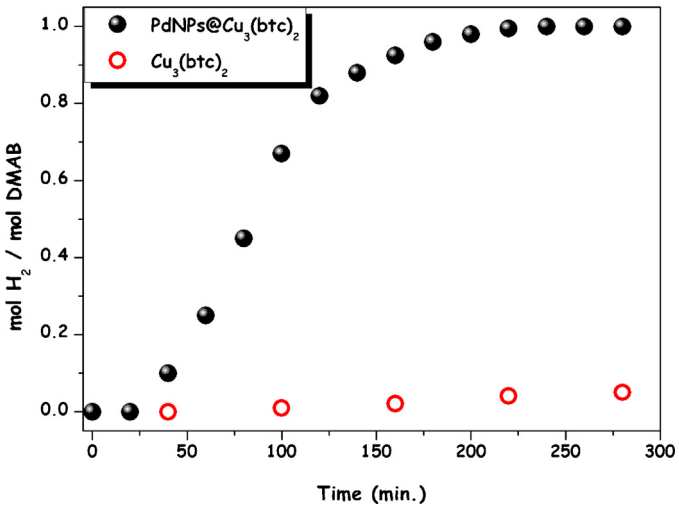

Fig. 6. Plots of mol H_2/mol DMAB versus time graph for the catalytic dehydrogenation of DMAB in toluene (100 mM DMAB in 10 mL toluene) starting with $Pd(acac)_2@Cu_3(btc)_2$ (100 mg with 0.86 wt% Pd loading corresponds to 8.1 μmol) and $Cu_3(btc)_2$ (100 mg) at room temperature.

3.2. Catalytic activity of activated $Cu_3(btc)_2$ and in-situ generated palladium(0) nanoparticles supported on $Cu_3(btc)_2$ framework ($PdNPs@Cu_3(btc)_2$) in the dehydrogenation of dimethylamine-borane

The *in-situ* generated $PdNPs@Cu_3(btc)_2$ catalyzed dehydrogenation of DMAB was followed by monitoring the hydrogen pressure and ^{11}B NMR spectroscopy. Before testing the catalytic activity of $PdNPs@Cu_3(btc)_2$ in the catalytic dehydrogenation of DMAB, the catalytic reactivity of the dehydrated host material $Cu_3(btc)_2$ was checked under the same conditions. The result of this experiment showed that palladium free $Cu_3(btc)_2$ is catalytically inactive in the dehydrogenation of DMAB (Fig. 6 circles). Fig. 6 (spheres) shows mol H_2/mol DMAB versus time graph for the catalytic dehydrogenation of DMAB starting with $Pd(acac)_2@Cu_3(btc)_2$ precatalyst at room temperature. It shows a sigmoidal-shaped kinetic profile characteristic of a heterogeneous process with an induction time period [13,38,39] prior to palladium(0) nanoparticles formation on the external surface of $Cu_3(btc)_2$. After an induction time period (~45 min) the hydrogen evolution starts immediately with an *initial* turnover frequency of 75 h^{-1} and continues until 1 equiv. of H_2 per mol DMAB is liberated. The apparent *initial* TOF value [40] of 75 h^{-1} is higher than that of all prior heterogeneous catalyst systems. Moreover, our *in-situ* generated $PdNPs@Cu_3(btc)_2$ provide better activity than the majority of the homogeneous catalysts tested in the dehydrogenation of DMAB (*see* Table 1). It should also be noted that the best activity values for both homogeneous and heterogeneous catalysis in the dehydrogenation of DMAB are achieved by using *in-situ* generated catalytic systems (see entries 15, 17, and 27 in Table 1).

^{11}B NMR spectra also shows complete conversion of $(CH_3)_2NHBH_3$ ($\delta = -12.8$ ppm) to $[(CH_3)_2NBH_2]_2$ ($\delta = 5$ ppm) [39] even at low Pd concentration ([Pd] = 0.81 mM, 0.81% mol catalyst) and room temperature.

3.3. Investigation of the heterogeneous nature of $PdNPs@Cu_3(btc)_2$ in the dehydrogenation of dimethylamine-borane

Although supported metal pre(catalysts) are accepted as heterogeneous catalysts for various transformations, it was conceivable

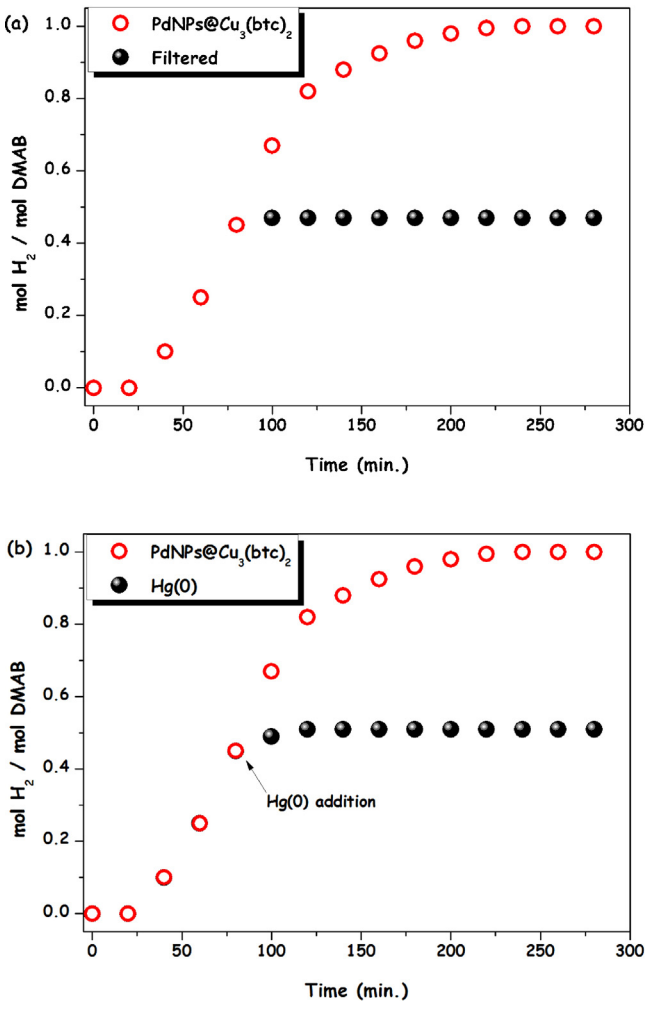

Fig. 7. Plots of mol H_2/mol DMAB versus time graph of (a) the filtration and (b) Hg(0) poisoning experiments for the catalytic dehydrogenation of DMAB in toluene (100 mM DMAB in 10 mL toluene) starting with $Pd(acac)_2@Cu_3(btc)_2$ (100 mg with 0.86 wt% Pd loading corresponds to 8.1 μmol) and $Cu_3(btc)_2$ (100 mg) at room temperature.

that the metal precursor ($Pd(acac)_2$ in our case) could be leached into solution, thus serving as a precursor to an active homogeneous species. In order to confirm the presence of a solely heterogeneous system, the effects of filtration and mercury (Hg(0)) poisoning experiments on the catalytic dehydrogenation of DMAB were carried out. Both control experiments are accepted tests for heterogeneous catalysts, with literature precedent for their use [44,51].

Two parallel reactions for the dehydrogenation of DMAB starting with $Pd(acac)_2@Cu_3(btc)_2$ were performed at room temperature. After 40% of conversion achieved, one mixture was filtered through glass fiber, the second was treated with excess Hg(0) (400 equiv.). Upon filtration, all visible bubbling in the solution stopped and hydrogen evolution was not observed (Fig. 7(a)) and the conversion of DMAB to cyclic product was shown and ceased immediately by ^{11}B NMR spectroscopy. Addition of Hg(0) to the reaction mixture provided almost identical results, completely halting catalysis (Fig. 7(b)). The ability of mercury(0) to poison heterogeneous metal(0) catalysts, which has little effect on most homogeneous systems, by amalgamating the metal catalyst or being adsorbed on its surface has been known for a long time [39,44,52,53]. These results are consistent with a catalyst, which is insoluble and heterogeneous.

3.4. Determination of activation energy (E_a) for the dehydrogenation of dimethylamine-borane catalyzed by in-situ generated PdNPs@$Cu_3(btc)_2$

Fig. 8(a) shows the plot of mol H_2/mol DMAB versus time graph for the catalytic dehydrogenation of DMAB starting with $Pd(acac)_2$@$Cu_3(btc)_2$ at four different temperatures. First of all, it is seen that the dehydrogenation rate of DMAB by PdNPs@$Cu_3(btc)_2$ catalyst increases (k_{obs} = 0.0075, 0.0095, 0.0167, 0.0279 ($\times 10^{-3}$ mol H_2/min) for 293, 298, 303, and 308 K, respectively) by the increase of temperature whereas the induction time periods (t_{ind} = 52, 38, 29 and 13 min for 293, 298, 303, and 308 K, respectively) required for the formation of active palladium(0) nanoparticles decrease. Secondly, Fig. 8(a) shows that PdNPs@$Cu_3(btc)_2$ formed *in-situ* during the dehydrogenation of DMAB can catalyze the reaction at complete conversion even at low temperature (293 K).

The observed rate constants (k_{obs}) determined from the nearly linear portions of the plots at four different temperatures were used for the plotting of Arrhenius graph (Fig. 8(b)) to calculate activation energy of 173.5 ± 16.2 kJ mol^{-1} for the *in-situ* generated PdNPs@$Cu_3(btc)_2$ catalyzed dehydrogenation of DMAB. This value is higher than that of previously found by Rh (34 kJ mol^{-1}) [39] and Ru (61.1 kJ mol^{-1}) [49] nanoparticles in the same reaction.

3.5. Isolability and reusability of PdNPs@$Cu_3(btc)_2$ in the dehydrogenation of dimethylamine-borane

The isolability and reusability of PdNPs@$Cu_3(btc)_2$ were also tested in the dehydrogenation of DMAB at room temperature. After complete dehydrogenation of DMAB in the first run, PdNPs@$Cu_3(btc)_2$ were isolated as powder by drying in vacuum and then bottled under an Ar atmosphere. Such isolated PdNPs@$Cu_3(btc)_2$ were found to be still active in the dehydrogenation of DMAB. They retain 80% of their initial catalytic activity (*initial* TOF = 60 h^{-1}) even at the fifth catalytic run, with complete conversion and generation of 1 equiv. H_2 under the same conditions as in the first run (Fig. 9(a) circles). The slight decrease (15%) in the fifth run may be attributed to the decrease in the number of active surface atoms due to the increase of the size of PdNPs due to their clumping. Indeed, a TEM image of PdNPs@$Cu_3(btc)_2$ the sample harvested after the fifth reuse shows an increase of the average size to 5.4 ± 1.1 nm (Fig. 9(b)). More importantly, Pd was not detected in the filtrate collected from each cycle by the ICP-MS technique (with a detection limit of 28 ppb for Pd) confirming that there is no leaching of PdNPs into reaction solution and retention of them on $Cu_3(btc)_2$.

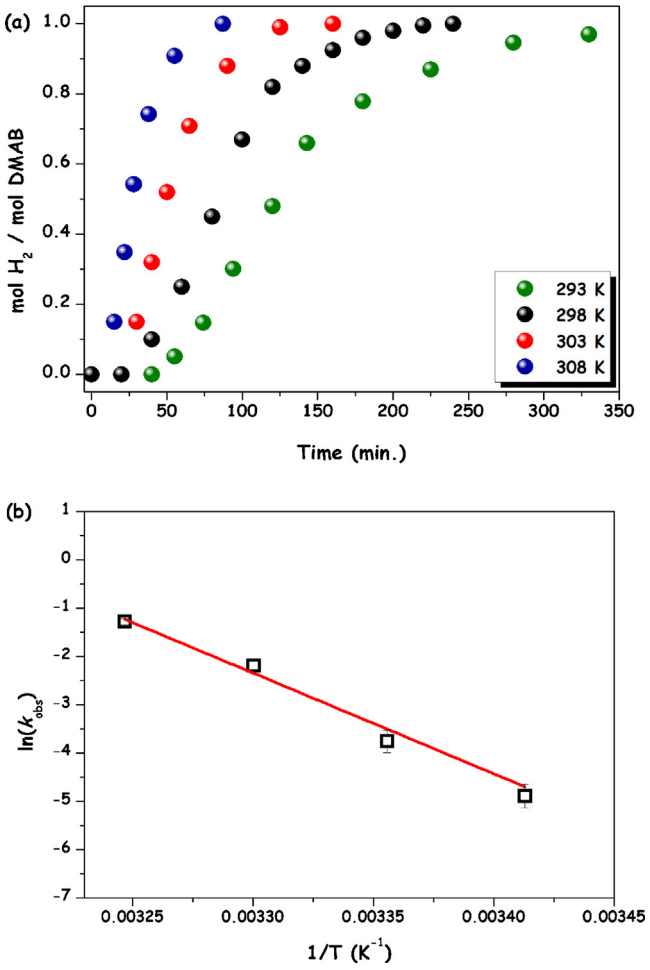

Fig. 8. (a) Plots of mol H_2/mol DMAB versus time graph for the catalytic dehydrogenation of DMAB in toluene starting with $Pd(acac)_2$@$Cu_3(btc)_2$ at different temperatures (293, 298, 303, 308 K) and (b) Arrhenius plot for the catalytic dehydrogenation of DMAB starting with $Pd(acac)_2$@$Cu_3(btc)_2$ ($y = (66.52 \pm 6.41) - (20869 \pm 1956)x$).

The reusability performance obtained by PdNPs@$Cu_3(btc)_2$ is better than that of previously reported by Ru-based nanocatalyst

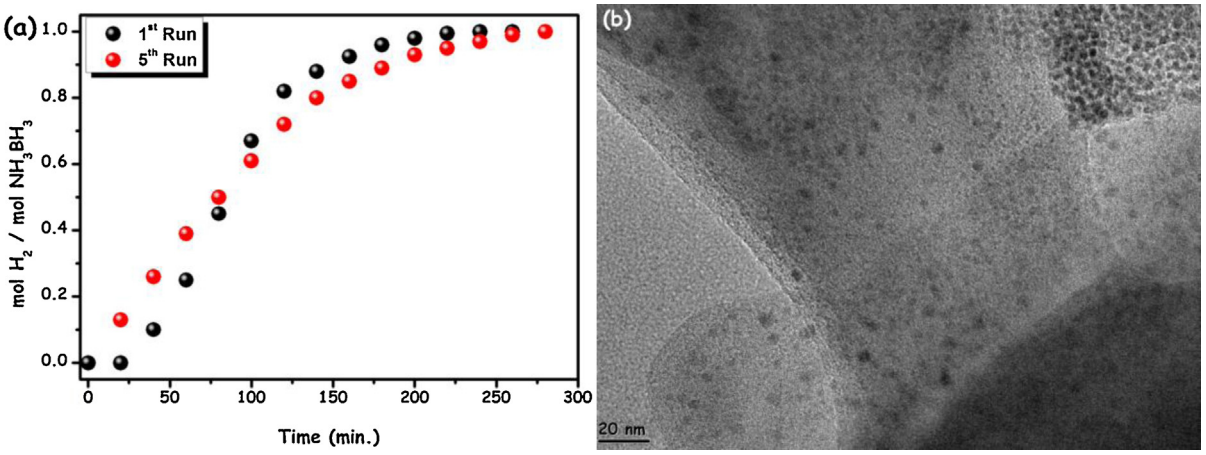

Fig. 9. (a) Plots of mol H_2/mol DMAB versus time graph for the catalytic dehydrogenation of DMAB in toluene starting with $Pd(acac)_2$@$Cu_3(btc)_2$ (black) and PdNPs@$Cu_3(btc)_2$ at the 5th catalytic run (red). (b) TEM image of PdNPs@$Cu_3(btc)_2$ sample harvested after the 5th catalytic run of the dehydrogenation of DMAB. (For interpretation of the references to colour in this figure legend, the reader is referred to the web version of this article.)

system [49] (*initial* TOF value of 45 h^{-1} at 3rd reuse by using 2.25 mol% catalyst, in our case *initial* TOF value is 60 h^{-1} at fifth reuse by using only 0.7 mol % catalyst) (*see* Table 1).

3.6. Catalytic lifetime of PdNPs@$Cu_3(btc)_2$ in the dehydrogenation of dimethylamine-borane

In a catalyst lifetime experiment started with $Pd(acac)_2$@$Cu_3(btc)_2$ (100 mg with 0.86 wt% Pd loading corresponds to 8.1 μmol), the *in-situ* generated PdNPs@$Cu_3(btc)_2$ were found to provide total turnover number (TTON) 2100 in the dehydrogenation of DMAB over 28 h before deactivation. This is a record value since the highest TTON known for the dehydrogenation of DMAB at room temperature is 1240 [49]. The XRD analysis of PdNPs@$Cu_3(btc)_2$ powder isolated at the end of the catalytic lifetime experiment shows the formation of amorphous $Cu_3(btc)_2$. The collapsing of $Cu_3(btc)_2$ throughout the lifetime experiment leads to agglomeration of surface bound PdNPs or sinking of them into collapsed framework. Both of these phenomena cause the deactivation of palladium nanoparticles catalysts.

4. Conclusions

In conclusion, PdNPs@$Cu_3(btc)_2$ were reproducibly prepared by the *in-situ* DMAB reduction of $Pd(acac)_2$@$Cu_3(btc)_2$ during the catalytic dehydrogenation of DMAB at room temperature. The characterization of this novel catalyst by using ICP-MS, P-XRD, XPS, TEM, HRTEM, STEM, STEM/EDX, HAADF/STEM, NMR spectroscopies and N_2-adsorption–desorption technique reveals the formation of well-dispersed palladium(0) nanoparticles of the size 4.3 ± 1.1 nm on the external surface of $Cu_3(btc)_2$ framework. The catalytic performance of PdNPs@$Cu_3(btc)_2$ in terms of activity, life-time and reusability was investigated in the catalytic dehydrogenation of dimethylamine-borane in toluene at room temperature. They show unprecedented catalytic activity among all the heterogeneous catalysts tested in the dehydrogenation of DMAB at room temperature providing an *initial* TOF value of 75 h^{-1} at complete conversion of DMAB to cyclic diborazane ($[Me_2NBH_2]_2$) and generation of 1 equiv. of H_2 per mole of DMAB. PdNPs@$Cu_3(btc)_2$ were also found to be highly stable against agglomeration and leaching throughout the catalytic runs in the dehydrogenation of DMAB, which make them highly reusable and long-lived catalyst. Palladium(0) nanoparticles supported on the external surface of metal organic framework retain almost their inherent catalytic activity (80%) even at the fifth catalytic reuse in hydrogen releasing from dimethylamine-borane. In addition to their superior activity and reusability performance, PdNPs@$Cu_3(btc)_2$ also provide an unprecedented catalytic lifetime measured in total turnover number (TTON = 2100) in the dehydrogenation of DMAB.

Understanding the existing synergistic effects between the metal and $Cu_3(btc)_2$ support remains an active area of research in our group. High catalytic activity, reusability and simple preparation and isolation procedures make PdNPs@$Cu_3(btc)_2$ a very attractive catalyst for performing selective dehydrogenation (or dehydrocoupling) reactions.

Acknowledgment

Partial support by Turkish Academy of Sciences is gratefully acknowledged.

References

[1] J. Shwarz, C. Contescu, K. Putyera, Encyclopedia of Nanoscience and Nanotechnology, 2nd ed., Marcel-Dekker, New York, 2004.
[2] D. Astruc, F. Lu, J.R. Aranzaes, Angew. Chem. Int. Ed. 44 (2005) 7852.
[3] M. Zahmakiran, S. Özkar, Nanoscale 3 (2011) 3462.
[4] S. Özkar, R.G. Finke, J. Am. Chem. Soc. 124 (2002) 5796.
[5] M. Zahmakiran, S. Özkar, Preparation of metal nanoparticles stabilized by the framework of porous materials, in: Sustainable Preparation of Metal Nanoparticles, RSC, London, 2013 (Chapter 3).
[6] J.Y. Lee, O.K. Farha, J. Roberts, K.A. Scheidt, S.T. Nguyen, J.T. Hupp, Chem. Soc. Rev. 38 (2009) 1450.
[7] D. Farrusseng, S. Aguado, C. Pinel, Angew. Chem. Int. Ed. 48 (2009) 7502.
[8] A. Corma, H. Garcia, F.X.L. Xamena, Chem. Rev. 110 (2010) 4606.
[9] A. Dhakshinamoorthy, H. Garcia, Chem. Soc. Rev. 41 (2012) 5262.
[10] J.J. Alcaniz, J. Gascon, F. Kapteijn, J. Mater. Chem. 22 (2012) 10102.
[11] S.S.-Y. Chui, S.M.F. Lo, J.P.H. Charmant, A.G. Orpen, I.D. Williams, Science 283 (1999) 1148.
[12] D.J. Tranchemontagne, J.R. Hunt, O.M. Yaghi, Tetrahedron 64 (2008) 8553.
[13] S. Çalışkan, M. Zahmakiran, F. Durap, S. Özkar, Dalton Trans. 41 (2012) 4976.
[14] R. Jelinek, S. Özkar, G.A. Ozin, J. Am. Chem. Soc. 114 (1992) 4907.
[15] J.M. Zamaro, N.C. Perez, E.E. Miro, C. Casado, B. Seoane, C. Tellez, J. Coronas, Chem. Eng. J. 195 (2012) 180.
[16] T. Ishida, M. Nagaoka, T. Akita, M. Haruta, Chem.-Eur. J. 28 (2008) 8456.
[17] J.Y. Ye, C.J. Liu, Chem. Commun. 47 (2011) 2167.
[18] Y.E. Cheon, M.P. Suh, Angew. Chem. Int. Ed. 48 (2009) 2899.
[19] C. Zlotea, R. Campesi, F. Cuevas, E. Leroy, P. Dibandjo, C. Volkringer, T. Loiseau, G. Ferey, M. Latroche, J. Am. Chem. Soc. 132 (2010) 2991.
[20] A. Staubitz, A.P.M. Robertson, I. Manners, Chem. Rev. 110 (2010) 4079.
[21] A. Staubitz, A.P.M. Robertson, M.E. Sloan, I. Manners, Chem. Rev. 110 (2010) 4023.
[22] D. Pun, E. Lobkovsky, P.J. Chirik, Chem. Commun. (2007) 3297.
[23] A.P.M. Robertson, R. Suter, L. Chabanne, G.R. Whittel, I. Manners, Inorg. Chem. 50 (2011) 12680.
[24] A. Aijaz, A. Karkamkar, Y.J. Choi, N. Tsumori, E. Rönnebro, T. Autrey, H. Shioyama, Q. Xu, J. Am. Chem. Soc. 134 (2012) 13926–13929.
[25] Q. Li, H. Kim, Fuel Process. Technol. 100 (2012) 43–48.
[26] G. Sirinivas, W. Travis, J. Ford, H. Wu, Z.-X. Guo, T. Yıldırım, Int. J. Mater. Chem. A 1 (2013) 4167.
[27] G. Sirinivas, W. Travis, J. Ford, H. Wu, Z.-X. Guo, T. Yıldırım, Int. J. Hydrogen Energy 37 (2012) 3633.
[28] L. Alaerts, E. Sguin, H. Poelman, F. Thibault-Starzyk, P.A. Jacobs, D.E. De Vos, Chem. Eur. J. 12 (2006) 7353.
[29] K. Schlichte, T. Kratzke, S. Kaskel, Microporous Mesoporous Mater. 73 (2004) 81.
[30] M. Zahmakiran, Dalton Trans. 41 (2012) 12690.
[31] Y. Xiong, J. Chen, B. Wiley, Y. Xia, J. Am. Chem. Soc. 127 (2005) 7332.
[32] I.P. Jones, Chemical Microanalysis Using Electron Beams, The Institute of Materials, London, 1992.
[33] C. Wagner, W.M. Riggs, L.E. Davis, J.F. Moulder, G.E. Muilenberg, Handbook of X-ray Photoelectron Spectroscopy, vol. 55, Physical Electronic Division, Perkin-Elmer, Eden Prairie, MN, 1979.
[34] G. Schmid, Clusters and Colloids: From Theory to Applications, VCH Publishers, New York, 1994.
[35] L. Guczi, D. Bazin, Appl. Catal. A: Gen. 188 (1999) 163.
[36] Y.-X. Jiang, W.-Z. Weng, D. Si, S.-G. Sun, J. Phys. Chem. B 109 (2005) 7637.
[37] S. Storck, H. Bretinger, W.F. Maier, Appl. Catal. A 174 (1998) 137.
[38] M.A. Watzky, R.G. Finke, J. Am. Chem. Soc. 119 (1997) 10382.
[39] M. Zahmakiran, S. Özkar, Inorg. Chem. 48 (2009) 8955.
[40] TOF value reported herein is not corrected for the amount of surface Pd atoms or the number of true active sites exists in the Pd nanoparticles.
[41] C.A. Jaska, K. Temple, A.J. Lough, I. Manners, Chem. Commun. (2001) 962.
[42] T.J. Clark, C.A. Russell, I. Manners, J. Am. Chem. Soc. 125 (2003) 9424.
[43] T.J. Clark, C.A. Russell, I. Manners, J. Am. Chem. Soc. 128 (2006) 9582.
[44] C.A. Jaska, I. Manners, J. Am. Chem. Soc. 126 (2004) 9776.
[45] M. Sloan, T.J. Clark, I. Manners, Inorg. Chem. 48 (2009) 2429.
[46] A. Friendrich, M. Drees, S. Schneider, Chem. Eur. J. 15 (2009) 10339.
[47] R.J. Keaton, J.M. Blacquiere, R.T. Baker, J. Am. Chem. Soc. 129 (2007) 11936.
[48] Y. Kawano, M. Uruichi, M. Shiomi, S. Taki, T. Kawaguchi, T. Kakizawa, H. Ogino, J. Am. Chem. Soc. 131 (2009) 14946.
[49] M. Zahmakiran, K. Philippot, S. Özkar, B. Chaudret, Dalton Trans. 41 (2012) 590.
[50] M. Zahmakiran, M. Tristany, K. Philippot, K. Fajerwerg, S. Özkar, B. Chaudret, Chem. Commun. 46 (2010) 2938.
[51] J.A. Widegren, R.G. Finke, J. Mol. Catal. A: Chem. 198 (2003) 317.
[52] G.M. Whitesides, M. Hackett, R.L. Brainard, J.P. Lavalleye, A.F. Sowinski, A.N. Izumi, S.S. Moore, D.W. Brown, E.M. Staudt, Organometallics 4 (1985) 1819.
[53] C.M. Hagen, J.A. Widegren, P.M. Maitliss, R.G. Finke, J. Am. Chem. Soc. 127 (2005) 4423.